

Performance and quality control of Clear-PEM detector modules

Pedro Amaral^a, Bruno Carriço^a, Miguel Ferreira^a, Rui Moura^{a,*}, Catarina Ortigão^a,
Pedro Rodrigues^a, José C. Da Silva^a, Andreia Trindade^a, João Varela^{a,b}

^aLIP, Av Elias Garcia 14, 1000-149 Lisboa, Portugal

^bIST, Av Rovisco Pais, 1049-001 Lisboa, Portugal

Available online 29 June 2007

Abstract

Clear-PEM is a dedicated PET scanner for breast and axilla cancer diagnosis, under development within the framework of the Crystal Clear Collaboration at CERN, aiming at the detection of tumors down to 2 mm in diameter. The camera consists of two planar detector heads with active dimensions $16.0 \times 14.5 \text{ cm}^2$. Each head has 96 Clear-PEM detector modules consisting of 32 LYSO:Ce pixels with dimensions $2 \times 2 \times 20 \text{ mm}^3$ packed in a 4×8 BaSO₄ reflector matrix compressed between two Hamamatsu S8550 APD arrays in a double-readout configuration for Depth-of-Interaction (DoI) determination.

The modules are individually measured and characterized before being grouped into Supermodules (comprised of 24 modules). Measured properties include photo-peak position, relative gain dispersion, energy resolution, cross-talk and DoI resolution. Optical inspection of matrices was also performed with the aid of a microscope, to search for pixel misalignments and matrix defects. Modules' performance was thoroughly evaluated with a 511 keV collimated beam to exactly determine DoI resolution. In addition, a fast quality control (QC) procedure using flood irradiations from a ¹³⁷Cs source was applied systematically. The overall performance of the 24 detector modules complies with the design goals of the Clear-PEM detector, showing energy resolution around 15%, DoI resolution of about 2 mm and gain dispersion among pixels of 15%.

© 2007 Elsevier B.V. All rights reserved.

PACS: 29.30.Kv; 29.40.Mc; 87.58.Fg; 87.59.Er

Keywords: Positron emission mammography; LYSO; APD; Energy resolution; Depth-of-Interaction; DoI resolution

1. Introduction

Clear-PEM is a dedicated PET scanner for breast and axilla cancer diagnosis, under development by a Portuguese R&D consortium, involving around 50 from 8 institutions with different areas of expertise ranging from physics, electronics and mechanics to imaging, software and medicine. This work is done within the larger framework of the Crystal Clear Collaboration at CERN [1].

The main goals of the project are low-dose exams and high spatial resolution. LYSO:Ce was chosen as scintillator due to its high gamma stopping power and fast decay time. Putting this together with a highly efficient, almost deadtimeless DAQ, fast- and low-dose exams can be

performed. To achieve high spatial resolution, the detector is highly pixilated and capable of measuring Depth-of-Interaction (DoI).

The scanner is a dual head plane detector with a total of 6144 LYSO:Ce ($2 \times 2 \times 20 \text{ mm}^3$) pixels arranged in 4×8 BaSO₄ reflector matrices. Optically coupled on each side of these matrices are 4×8 Hamamatsu S8550 APD arrays ($1.6 \times 1.6 \text{ mm}^2$ pixel size) in a double-readout configuration which enables extraction of DoI information through signal amplitude asymmetry at each pixel end. The active area dimension is $16.0 \times 14.5 \text{ cm}^2$ for each detector plate, which results in a channel density of approximately 26 channels/cm² [2].

Structurally the detector is assembled starting with the mentioned 4×8 matrices, which are mounted in pairs in double-modules' mechanical housing boxes. Twelve of these boxes are grouped in fully functional electro-

*Corresponding author.

E-mail address: moura@lip.pt (R. Moura).

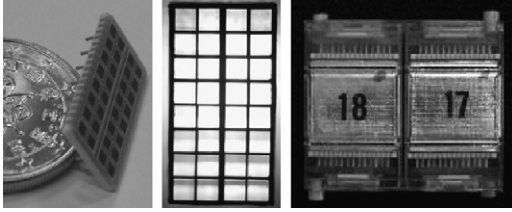


Fig. 1. Left: Hamamatsu S8550 APD. Center: optical inspection of a retro-illuminated crystal matrix. Right: assembled double module.

mechanical structures with front-end electronics boards. Four clones of these Supermodules are put side by side to make the detector plates (Fig. 1).

2. Performance evaluation with collimated 511 keV beam

Before assembling, the large number of modules required to make the detector; module performance needs to be evaluated. In this phase, particular emphasis is given to DoI determination and top–bottom APD pixel calibration, since these are harder to evaluate when modules are grouped in larger sets. For this purpose, the setup described below was used.

2.1. Collimated beam setup

To collimate, the annihilation gammas from a Na-22 positron source in the crystal, the coincidence trigger of the opposing gamma photon is considered. This eliminates Comptons and secondaries created when using lead collimators. To perform this electronic collimation of the 511 keV gamma-ray beam, the setup in Fig. 2 is used. The distance between the radioactive source and the module is made as small as possible (~ 1 cm) while the distance to the NaI:Tl is large (~ 40 cm), limited mainly by the rate of events in coincidence with the module.

The beam is collimated perpendicularly to the long axis of the crystals and is incident between 2 rows of 8 crystals, so that 16 crystals are measured at each beam position. The width of the beam is approximately 1.5 mm. Five different equidistant positions along the crystals' long axis are acquired: 8 (near top APD), 4, 0 (crystal center), -4 and -8 mm (near bottom APD). The true coincidence rate is about 250 Hz of which nearly 9% are randoms. Electronic threshold is placed between 100 and 150 keV and noise averages 6.5 keV for all channels. APDs are operated at multiplication gain 50 and temperature is kept around 20°C during measurements.

2.2. Calibration

Inter-calibration of top and bottom readout chains, as well as the usual overall energy and DoI, calibration is needed. The chosen calibration procedure tries to balance gains on the top and bottom APD, by applying a suitable constant (k) to the bottom APD signal, so that photo-

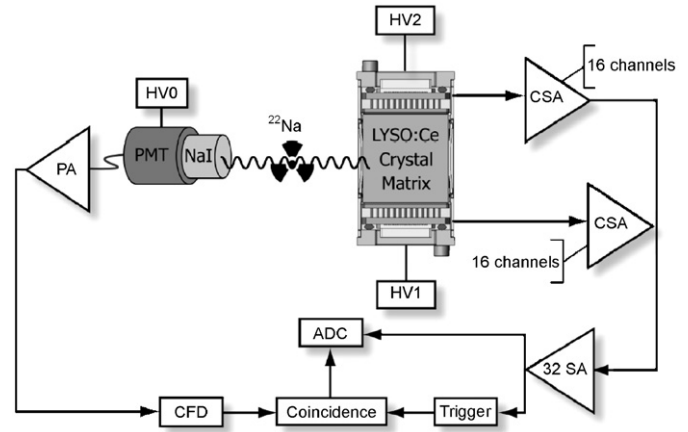


Fig. 2. Setup for electronic collimation of the 511 keV photons.

peaks at equivalent positions have the same amplitude seen by the top and bottom APD. The resulting estimators for energy and asymmetry on an event-by-event basis are:

$$E = \text{Top} + k \times \text{Bot}$$

$$A = \frac{\text{Top} - k \times \text{Bot}}{\text{Top} + k \times \text{Bot}}$$

where Top means ADC counts after pedestal subtraction for the signal collected on the top APD and Bot is the same for the bottom APD.

2.3. Photo-peak and energy resolution

A Gaussian on top of a linear background is fitted to the 511 keV photo-peak to extract photo-peak amplitude and energy resolution. The amplitude of the peak includes the light yield of the crystal along with the optical coupling to the APD pixel and its gain, as well as the gain of the readout chain.

The average amplitude of the 511 keV photo-peak in the 32 pixels at all beam positions is 1487 ± 153 ADC counts (see right of Fig. 3). Energy resolution distribution (see left of Fig. 3) for the same measures is $15.6 \pm 1.3\%$, which is well within expectations for such small pixels [5–7].

2.4. Asymmetry and DoI

At each beam position, the asymmetry variable is histogrammed and fitted by a Gaussian (see Fig. 4). The average asymmetry, hence, obtained for each position is plotted against the known DoI coordinate and a linear fit is applied to extract the slope m that converts asymmetry A into DoI coordinate through: $\text{DoI}(\text{mm}) = A(\%) / m(\%/ \text{mm})$.

FWHM of these Gaussian distributions are the DoI resolutions at each position, whose distribution is represented on the right of Fig. 4 for all pixels. DoI resolution includes the dispersion of scintillation photons as well as the beam width (> 1.5 mm as described in Section 2.1). Average DoI resolution for all measures is 2.23 ± 0.21 mm which matches the 2×2 mm² transverse pixel dimensions [6,7].

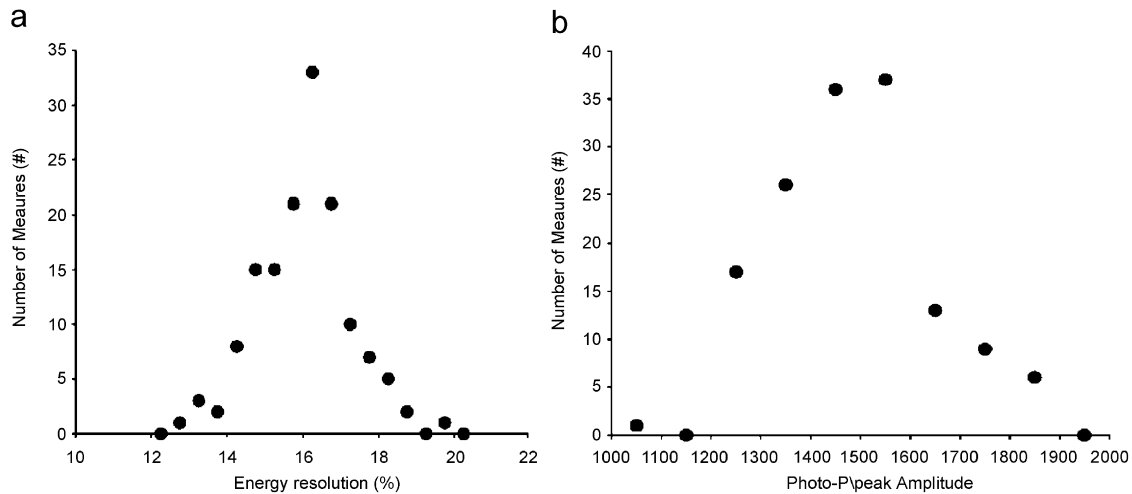


Fig. 3. Energy resolution and photo-peak amplitude distributions for the five incidence positions for each pixel.

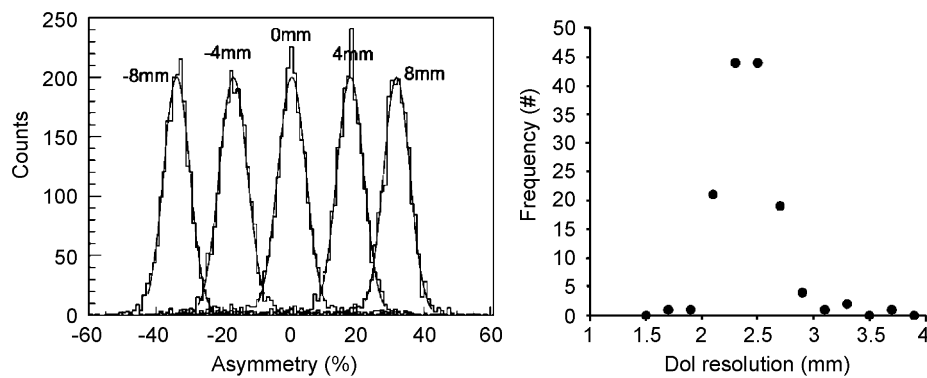


Fig. 4. Left: asymmetry peaks at each beam position for one pixel. Right: DoI resolution distribution for all measures.

3. Quality control with ^{137}Cs

To perform an exhaustive quality control (QC) of the first 24 Clear-PEM modules to be assembled in a Super-module, fast irradiation floods with a ^{137}Cs source and automated analysis tools were used. Module properties' stability with time was also investigated [3].

The setup used is essentially the same described in Fig. 2 without the NaI:Tl branch previously used as coincidence trigger.

APDs undergone a thorough quality control process and were characterized individually as described in Ref. [4].

3.1. Relative gain

Relative gain is defined as the photo-peak amplitude of a pixel normalized by the average of all measures made with the same readout chain, to eliminate electronic amplification differences from the results, emphasizing differences due to crystal's light yield, optical couplings and APD pixel's gain.

Overall relative gain has a distribution centered at 1 as expected by construction and a standard deviation of 13% (see Fig. 5), which poses no problems in terms of

calibration and makes gain compensation (through bias voltage, for example) unnecessary.

3.2. Energy resolution

Energy resolution for the 662 keV photo-peak is good for pixels this small, with a value of $13.4 \pm 1.3\%$, having all the 768 pixels (32 pixels/matrix \times 24 matrices) into account (see Fig. 5).

3.3. Asymmetry per unit length

As referred in Section 2.4, to extract the DoI coordinate one must determine the conversion slope that gives the variation in asymmetry (%) for a given variation in impact point (mm). Using floods, we do this by assuming the maximum variation in asymmetry corresponds to the full-width at one-third of the average height of the asymmetry distribution plateau for photo-peak events. This width divided by the crystal length is the conversion constant in %/mm (see left of Fig. 6). It is desirable that this constant is high, so that there is fine precision in the conversion of the asymmetry to DoI coordinate. The distribution of these values for all pixels is shown at the right of Fig. 6, which

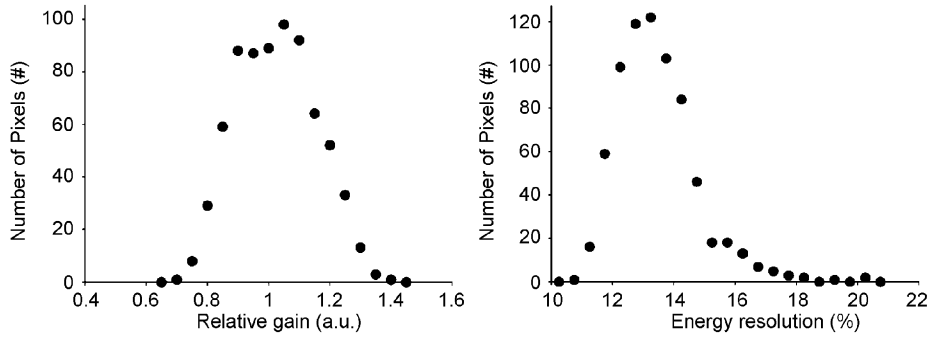


Fig. 5. Relative gain and energy resolution distributions for all pixels in all 24 matrices.

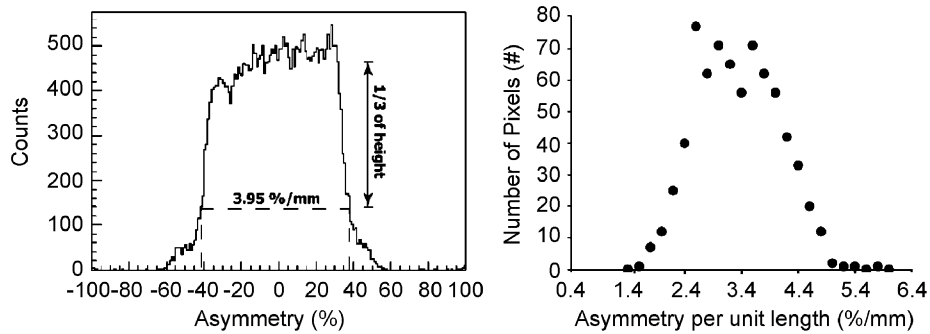


Fig. 6. Left: asymmetry histogram for photo-peak events in one pixel. Right: asymmetry per unit length distribution.

presents a mean value of 3.26%/mm with a standard deviation of 0.71%/mm.

3.4. Cross-talk

Cross-talk is determined by selecting photo-peak events in a central pixel and looking at reminiscent energy deposits in neighboring pixels. The ratio of the mean value of the peak formed by these deposits to the photo-peak amplitude is assumed to be the cross-talk. Average for all measured pixels is $2.5 \pm 1.0\%$ which is well within expectations.

4. Conclusions

Performance of Clear-PEM modules was evaluated through a series of measures with a collimated 511 keV gamma-ray beam, showing that the desired global detector goals for fast and high-resolution mammography exams can be achieved. Namely, the 15.6% energy resolution and 2.2 mm DoI resolution are in agreement with the designed aims of the project [2], showing the very good performance of the detector module [5–7].

The great number of pixels makes the modules' quality control an essential tool before assembly. A simple, fast, mostly automatic procedure was developed to test all the modules and control their performance. Stability issues were also investigated and no worries arose from these

studies [3]. Overall results show that the gain dispersion is small (13%) and partly due to the APD pixels' gain dispersion [4]. Energy resolution at 662 keV (13.4%) is compatible with that at 511 keV if we apply the $1/\sqrt{E}$ correction. The inter-pixel cross-talk in the Clear-PEM detector modules is smaller than 3%, requiring no additional redesign considerations.

Acknowledgments

This work was supported by the Innovation Agency (AdI) and the Operational Program for Information Society (POSI), Portugal. The work of P. Amaral, B. Carriço and C. Ortigão was supported by AdI. The work of R. Moura, P. Rodrigues and A. Trindade was supported by the Fundação para a Ciência e a Tecnologia.

References

- [1] P. Lecoq, J. Varela, Nucl. Instr. and Meth. A 486 (2002) 1.
- [2] M.C. Abreu, et al., IEEE Trans. Nucl. Sci. NS-53 (1) (2006) 71.
- [3] C. Ortigão, et al., Long-Term Stability of the Clear-PEM Detector Modules, EuroMedIm 2006, Marseille, France, 9–12 May 2006.
- [4] B. Carriço, et al., Characterization and Quality Control of Avalanche PhotoDiode Arrays for the Clear-PEM Detector Modules, IWORID 2006, Pisa, Italy, 2–6 July 2006.
- [5] U. Heinrich, et al., Nucl. Instr. and Meth. A 486 (2002) 60.
- [6] J.S. Hubber, et al., IEEE Trans. Nucl. Sci. NS-48 (2001) 684.
- [7] E. Gramsch, et al., IEEE Trans. Nucl. Sci. NS-50 (3) (2003) 307.